1550 (1970).
[20]S. Meiboom and R. C. Hewitt, Phys. Rev. Lett. 30, 261 (1973).
[21]R. S. Pindak, C. C. Huang, and J. T. Ho, Phys. Rev. Lett. 32, 43 (1974), and Solid State Commun. 14, 821 (1974).
[22]V. N. Tsvetkov, Acta Physicochim. U.R.S.S. 10, 555 (1939).
[23]This estimate of C is obtained by substituting $K_{11} = 10^{-6}$ dyne, $\rho = 1$ g cm^{-3}, and $\xi_0 = 10$ Å into Eqs. (6.6) and (6.7) of Ref. 3. The estimate $C = 10^{-2}$ P in Eq. (6.8) of Ref. 3 appears to be a numerical error.

Theory and Experiments on Configurations with Cylindrical Symmetry in Liquid-Crystal Droplets

M. J. Press and A. S. Arrott
Department of Physics, Simon Fraser University, Burnaby, British Columbia, Canada V5A 1S6
(Received 13 May 1974)

Elasticity theory is applied to nematic liquid crystals with particular boundary conditions. The calculus of variations is used to derive the torque equations, the solutions of which are found by relaxation methods on a digital computer. These solutions are used to draw pictures of the molecular arrangements and with the aid of Maxwell's equations to predict the observed optical patterns, including the case of magnetic fields applied along the symmetry axis.

We have obtained agreement between elastic continuum calculations and optical patterns observed with crossed polarizers in nematic liquid-crystal droplets. We started with the simple question: What is the minimum-energy configuration of a drop in which the molecules within the drop tend to be parallel to one another, yet are pinned at a definite angle to the surface of the drop? It is a simple conclusion that these drops should show surface singularities of molecular size in extent, and that a cylindrically symmetric solution would put the singularities (point disclinations) at the north and south poles of the drops. To observe the molecular configurations about these poles we floated droplets on the surface of water. This procedure has the three important advantages that the droplets are lens shaped resulting in better optics than obtained with spheres, the water provides a very homogeneous and reproducible substrate which for many liquid crystals gives droplets with cylindrical symmetry in the molecular alignment, and for methoxybenzylidene butylaniline (MBBA, the liquid crystal we use most often) the drops remain in the nematic state for many hours despite some gradual absorption of water. Figure 1 shows three droplets similarly prepared and of similar size which when viewed between crossed polarizers exhibit three distinct patterns: a right-handed, a left-handed, and a normal configuration. Similar patterns have been observed for almost a century, with Lehman[1] devoting a lifetime to such studies. The theory of such observations has received little attention despite the possibility that such a macroscopic element with three states might have some technological interest.

The successful analysis of this problem yields the computer graphics of Figs. 2 and 3 for the orientation of the molecules. To obtain the opti-

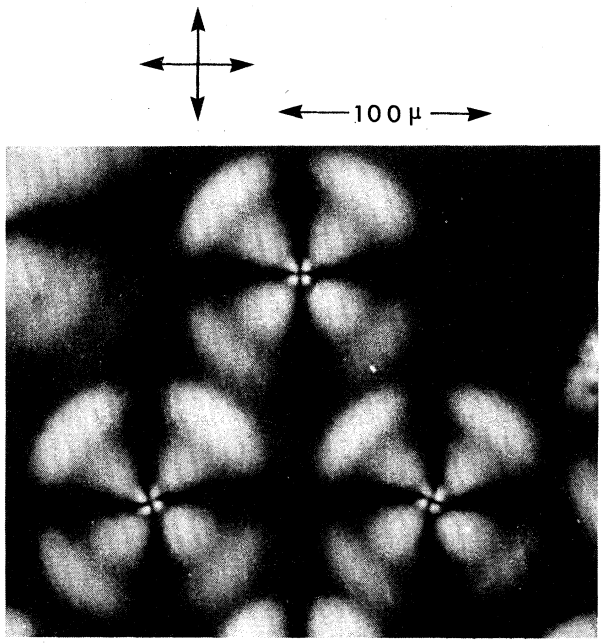

FIG. 1. MBBA droplets on a water substrate observed between crossed polarizers with white light displaying the three different configurations.

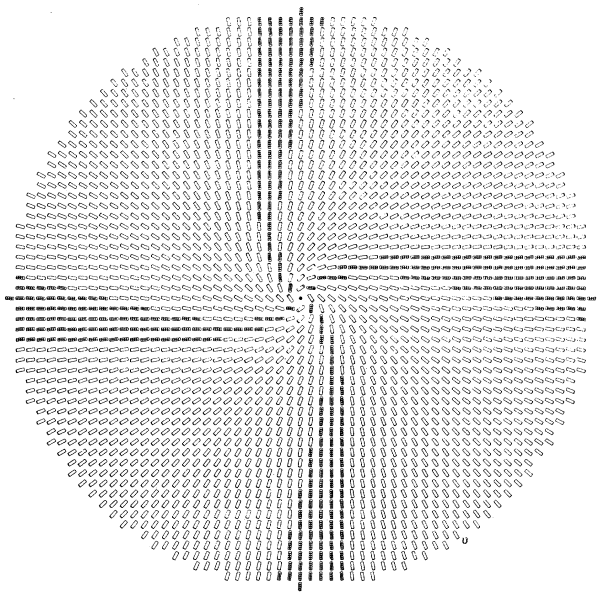

FIG. 2. View of a layer in the ρ-φ plane just below the water surface for the twisted configuration with $S/B=0.8$ and $T/B=0.5$ with $\rho_0/z_0=4$. The inserted crosses indicate those molecules whose projections in the ρ-φ plane lie within 7° of either the polarizer or the analyzer axis.

cal patterns observed with the droplets between crossed polarizers one should solve Maxwell's equations in the medium. This is carried out under the assumption of local translational invariance in the plane perpendicular to the light path.[2] This assumption is not quite adequate at the center of the droplets, but nevertheless is sufficiently valid to yield agreement between theory and experiments for the molecular configurations. Crudely one can see the effect by considering a representative slice parallel to the water substrate near the water interface as in Fig. 2. Where the light is polarized parallel or perpendicular to the projections of the molecules, its polarization is maintained and it is absorbed in the analyzer. The result is the "brush" pattern indicated by the darkened molecules. The brush pattern referred to as the normal configuration corresponds to the molecules confined to the radial-vertical plane.

The principal source of the problem is that the boundary conditions are not compatible with the vanishing of the derivative in the bulk. For the water interface the molecules are pinned to lie in the surface. For the air surface the molecules are pinned to lie in a cone making an angle of 15 deg between the molecular axis and the normal to the surface. Minimization of the energy in the bulk proceeds primarily by a process which is here termed "splay canceling". A radial component of the directrix produces a term in the divergence which offsets the contribution to the divergence from the variation in the directrix from the top surface to the bottom surface.

The elastic continuum theory starts with a directrix $\hat{n}$ which describes the mean orientation of the molecules at each point. The energy in the bulk is given by[3]

$$E=\pi\iint d\rho\, dz[S|\nabla\cdot\hat{n}|^2+T|\hat{n}\cdot(\nabla\times\hat{n})|^2+B|\hat{n}\times(\nabla\times\hat{n})|^2]\rho, \quad (1)$$

where cylindrical symmetry has been imposed in correspondence to the direct observation that rotation of the drops between crossed polarizers causes no change in the optical patterns. S, T, and B refer to the splay, twist, and bend elastic constants, respectively.

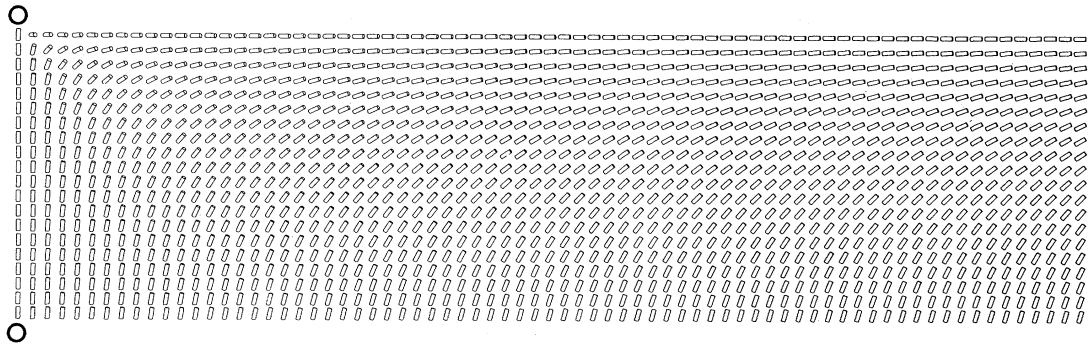

FIG. 3. The molecules in the ρ-z plane of the twisted configuration with $S/B=0.8$ and $T/B=0.5$ with $\rho_0/z_0=4$. OO is the axis of symmetry.

With the directrix expressed in terms of the usual two polar angles θ and φ and using the cylindrical coordinates ρ and z, one finds that the energy expression contains 24 terms, or 25 when we include the effect of a magnetic field along the symmetry axis. A typical set of three terms is

$$\rho \sin^2\theta\, \varphi_\rho{}^2(S\sin^2\varphi + T\cos^2\theta\cos^2\varphi + B\sin^2\theta\cos^2\varphi),$$

where φ_ρ is a partial derivative.

Carrying out the calculus of variations produces two torque equations, one with 31 and the other with 27 terms plus boundary conditions. The torque equations are simultaneous nonlinear second-order partial differential equations. The solutions we report here are for the simple case where the upper and lower boundaries are flat, horizontal, and separated by a distance z_0, and the outside boundary is cylindrical, vertical, and at $\rho = \rho_0$. We use hard pinning on the horizontal boundaries. On the upper one we take $\theta = \pi/2$, with φ to be determined from a first-order nonlinear partial differential equation with 5 terms, while on the lower one we take $\theta = \pi/12$, again with φ to be determined from this partial differential equation. On the outside surface we use free boundary conditions, and thus two simultaneous first-order partial differential equations, each with 8 terms, must be satisfied here. The choice of $\theta = \pi/2$ corresponds to the water–liquid-crystal interface with the liquid-crystal molecules strongly attracted to the polarizable water. The choice of $\theta = \pi/12$ corresponds roughly to the observed behavior of MBBA at an air interface.[4] The free boundary conditions at $\rho = \rho_0$ are an approximation that produces a small amount of artifice into the behavior near $\rho = \rho_0$. But we are concerned primarily with the behavior over the central "flat" portion of the drop, so this is of little consequence.

Our assumptions of a flat surface, of hard pinning at other than $\theta = 0$, and of cylindrical symmetry are not compatible at the center of the surface. We treat this part of the problem in detail elsewhere. Here it is sufficient to say that on the scale of 100 nm to 100 μm in which we treat the present problem it is adequate to ignore the details of how the infinite energy density of the singularity is relaxed.

The torque equations with the above boundary conditions have been solved by relaxation methods using typically a grid of 30 by 39 points, with variable grid spacing, becoming finer near the boundaries and the z axis. The relaxation is adequate after 1000 to 2000 passes. We have results for $\rho_0/z_0 \simeq 2$, 4, and 8 for several values of the ratios B/S and T/S. The behavior of the region $\rho < 2\rho_0$ becomes independent of ρ_0/z_0 for $\rho_0/z_0 > 4$. At $\rho = 2z_0$ the θ values are within 1% of the values calculated for $\rho \to \infty$. For $T/S \geq 1$ we find the normal configuration which has $\varphi = 0$ everywhere. For $T/S \leq 0.9$ we find the three solutions which we are seeking. The degree of rotation of the cross decreases with increasing T/S for $T/S \leq 0.9$. The two solutions with handedness, which are mirror images of each other about $\varphi = 0$ with the same energy, differ from the normal solution primarily in the φ values. The θ values are quite close. The energy of the normal solution, while higher, is only slightly higher. Extrapolation to infinite radius suggests that the energy difference is no more than 10^{-9} erg for the whole drop (for $T = 0.4$ μdyn, $S = 0.65$ μdyn, and $B = 0.8$ μdyn which are suitable choices for MBBA[5]).

A much more important saving in energy common to all three cases occurs in the cancelation of two terms in the divergence:

$$\mathrm{div}\hat{n} = [\sin\theta(\cos\varphi)/\rho - \sin\theta\,\theta_z + \ldots].$$

This cancelation occurs for $\varphi = 0$, but not for $\varphi = \pi$ (also a solution) in the case where θ_z is positive as it is here. It is this that requires φ to go to zero as the terms in θ_ρ and φ_ρ become negligible at larger radius. It should be recalled that θ_z remains large because of the conflicting boundary conditions. That this cancelation is most effective when $\rho \sim z_0$ results in a minimum in the energy density in this region, and even the total energy per unit area of the drop goes through a minimum with increasing radius. Thus there is a possibility that a large-area layer might achieve lower energy by supporting an array of point disclinations.

We have also studied the effects of vertical magnetic fields both under the microscope and on the computer and have obtained quantitative agreement.

The full equations, the optical calculations, the comparison of theory and experiment, and the details of the phase diagram will be reported elsewhere.

We wish to acknowledge the helpful advice of Dr. R. D. Russell concerning relaxation methods and the encouragement of Professor P. G. de Gennes in the initial stages of this work. This research has been supported by the National Re-

search Council of Canada.

[1]O. Lehman, Ann. Phys. (Leipzig) 66, 323 (1921).
[2]The calculation of S. C. Chou, L. Cheung, and R. B. Meyer, Solid State Commun. 11, 997 (1972), has been expanded to allow the molecules complete freedom in their orientations.
[3]F. C. Frank, Discuss. Faraday Soc. 25, 19 (1958).
[4]M. A. Bouchiat and D. Langevin-Cruchon, Phys. Lett. 34A, 331 (1971).
[5]I. Haller, J. Chem. Phys. 57, 1400 (1972).

g Tensors and Tensor Interactions—Their Effect on Conduction-Electron Spin Resonance*

M. B. Walker
Department of Physics and Scarborough College, University of Toronto, Toronto M5S 1A7, Ontario, Canada
(Received 1 April 1974)

Conduction-electron g tensors depending on electron momentum can (through the cyclotron motion of the electron) cause transitions between spin Zeeman levels which broaden and shift the conduction-electron spin resonance. Tensor quasiparticle interactions are capable of similar effects. The relaxation time and exchange parameter controlling motional and exchange narrowing of the conduction-electron spin resonance are precisely defined.

Lubzens, Shanabarger, and Schultz[1] have recently reported detailed measurements of the frequency dependence, temperature dependence, and dependence on resistivity ratio of the g value and linewidth of conduction-electron spin resonance (CESR) in aluminum. The initial report[2] of CESR in aluminum led Dupree and Holland[3] to suggest that g anisotropy might be important, and theories of motional and exchange narrowing of g anisotropy have been formulated by de Botton[4] and Fredkin and Freedman.[5] The results of Lubzens, Shanabarger, and Schultz[1] fit very well the predictions of these latter theories.[4,5]

In the present work, the tensor nature of the g value is explicitly considered (for the first time) and such considerations lead to new processes affecting the linewidth and g shift of the CESR. In the light of this development, a reinterpretation of the results of Lubzens, Shanabarger, and Schultz[1] would be useful, as it is believed that these new results may strongly affect the value of the parameter B (defined below).

Also, the motional-narrowing relaxation rate is given in terms of a weighted average of the impurity scattering cross section,[6] the weighting factor being different from that determining the resistivity relaxation rate. Similarly, the exchange parameter B controlling exchange narrowing is precisely defined.

Finally, we follow up a remark of de Botton[4] that the influence of spin-orbit coupling on the quasiparticle interaction can produce effects qualitatively similar to those produced by g anisotropy. A new type of tensor quasiparticle interaction is introduced and is shown to give rise to contributions to the effective g tensor. Nothing is presently known about the magnitude of such tensor interactions, but it is known that the magnitude of the g anisotropy required to account for the aluminum results is surprisingly large.[1] A first-principles estimate of the magnitude of the tensor interaction would thus be of value.

We shall study in detail an isotropic electronic Fermi liquid. For a Zeeman Hamiltonian of the form $H_Z = -g(\vec{p})\mu_B \vec{s}\cdot\vec{H}$ to be invariant with respect to simultaneous rotations of $\vec{s}$, $\vec{H}$, and $\vec{p}$, we must have $g(\vec{p})$ independent of the direction $\vec{p}$. Anisotropy in g can only be introduced by the use of a g tensor, and we therefore assume a Zeeman Hamiltonian

$$H_Z = -\mu_B \vec{s}\cdot\overleftrightarrow{g}\cdot\vec{H}, \quad \overleftrightarrow{g} = g_0\overleftrightarrow{1} + \tfrac{1}{2}g_2\overleftrightarrow{T}, \tag{1}$$

$$\overleftrightarrow{T} = 3\vec{p}\vec{p} - \overleftrightarrow{1}. \tag{2}$$

The quantity $\overleftrightarrow{1}$ is the unit dyadic, and $\vec{p}$ denotes a unit vector in the direction of the electron momentum.

The tensor part of the Zeeman interaction can be written in the form $-g_2\mu_B\vec{s}\cdot\vec{H}_{\rm eff}$, where $\vec{H}_{\rm eff}$ is an effective magnetic field given by $\vec{H}_{\rm eff} = \frac{1}{2}[3\vec{p}(\vec{p}\cdot\vec{H}) - \vec{H}]$. The effective field has a component in the direction of the momentum of the electron, as well as a component along the ex-

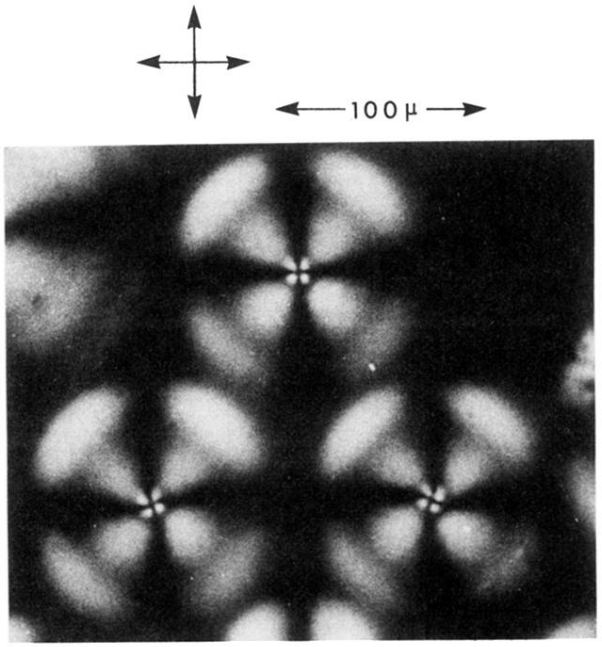

FIG. 1. MBBA droplets on a water substrate observed between crossed polarizers with white light displaying the three different configurations.